QUALITY OF MMS FORWARD-PHOTOGRAPHED IMAGE INTERSECTION

Wen-Hau Lan[1] , Jaan-Rong Tsay[2], and Yen-Ting Lee[3]
[1]Graduate Student, Department of Geomatics, National Cheng Kung University,
1 University Road, Tainan, 70101 Taiwan; Tel: +886-6-2757575 ext. 63834,
E-mail: b11050713@msn.com

[2]Associate Professor Dr.-Ing., Department of Geomatics, National Cheng Kung University,
1 University Road,Tainan, 70101 Taiwan; Tel: +886-6-2370876 ext. 838,
E-mail: tsayjr@mail.ncku.edu.tw

[3]Graduate Student, Department of Geomatics, National Cheng Kung University,
1 University Road, Tainan, 70101 Taiwan; Tel: +886-6-2757575 ext. 63834,
E-mail: nm1377@yahoo.com.tw

KEY WORDS: MMS, Intersection, Reliability, Error ellipse

ABSTRACT: This paper studies the quality of object point positioning by means of image intersection by using close-range images forward taken on a land-based MMS van driving along a street. Due to the weak geometry of intersection of multiple corresponding image rays, photo triangulation often diverges or provides worse results. Nevertheless, the problems can be solved so that the positioning accuracy still suits for updating 1/1000 maps. Tests are done by using different sets of images with diverse baseline lengths, constraint data, image point distributions, and different number of images. All corresponding image points are measured either by SIFT or manually. In each photogrammetric intersection network, the geometric strength figures are analyzed such as inner reliability, lengths and directions of semi-axes of error ellipses, as well as the standard deviations of ground coordinates. Also, a number of ground check points are used to evaluate the quality of the results. They demonstrate that, under a proper constraint configuration, the positioning technique is available for cartography of 1/1000 maps. For example, by using three full control points, the average accuracy of ground coordinates reaches 9~15cm.

1. INTRODUCTION

Along with dramatically increasing demand on spatial information, the Mobile Mapping Systems (MMS) play an alternative role for collecting spatial data. MMS contains different platforms such as satellites, airplanes and automobiles. Among these, satellites and airplanes suit for spatial data acquisition in larger areas, however they are not economic systems for small areas. Moreover, there will be a problem of occlusion when aerial or spaceborne photogrammetry is used to produce or update maps and Digital Terrain Models (DTMs). Nevertheless, the problems mentioned above can be solved by automobiles-carrying MMS in an economical manner.

In practice, if terrestrial or close-range images are forward taken on such a MMS van driving along a street, due to the weak geometry of intersection of multiple corresponding image rays, photo triangulation often diverges or provides worse results. The solutions to these problems are studied in this paper.

In 1993, the Ohio State University (OSU), USA, published first a land-based Mobile Mapping System (MMS), called GPSVan (Lee et al., 2004). The GPSVan includes two monochrome digital cameras and two Video Home System (VHS) cameras. It was able to achieve the absolute object space accuracies of 1~3m(Ellum and El-Sheimy, 2002). After the GPSVan, more and more MMSs are then developed and applied increasingly. For example, in 1994, the first generation VISAT(Video cameras, an Inertial system, and SATellite GPS receivers) was produced at the University of Calgary, Canada. The second generation VISAT included 8 monochrome digital cameras and 1 VHS camera. Its absolute object space accuracies was 0.3m for points within 35m radius while moving at a speed of 60km/hr(EI-Sheimy, 1996). The third generation VISAT, VIAST 2006™, included 6 monochrome CCD digital cameras, 1 colour VHS camera and laser scanner.

This paper focuses on MMS forward-photographed image triangulation network analysis. Due to the size the general van, the baseline lengths between two forward-photographed cameras are shorter generally. In our test data, both forward-photographed cameras have the baseline length 1.65m. It makes the parallactic angles of object points smaller, and results in a weak photogrammetric intersection network. The following three experiments are analyzed: 1. The test images are taken on a MMS van driving along a street to a forward direction. Its geometry of intersection is different from aerial photogrammetry. Therefore, some tests are done to analyze whether the accuracy of object coordinates determined in photo triangulation or image intersection using the aforementioned images still suits for cartography of 1/1000 maps when adding different number of full control points. 2. When adding different number of full control points and GPS(Global Positioning System)/IMU(Inertial Measuring Unit) data, the quality and its applicability for cartography of 1/1000 digital topographic maps is analyzed. 3. When updating 1/1000 maps, only a few images pairs and less image points are adopted. In this case, the quality of determined object coordinates is studied, and also its applicability for 1/1000 cartography is analyzed.

2. TEST DATA

Table 1 lists the parameters of both MMS forward-photographed cameras with the baseline length 1.65m. Figure 1 illustrates both images of the close-range image pair taken with the forward-photographing camera No.1 and No. 2 along the street in the test area.

Table 1. Parameters of both MMS forward-photographed digital cameras

Camera Parameters	x_0(mm)	y_0(mm)	f(mm)	Image Size(pixels)	Pixel Size(mm)	FOV (°)
Camera No. 1	0.139	-0.046	8.25	1392 x1040	0.00645	68
Camera No. 2	-0.014	-0.067	8.27	1392 x1040	0.00645	68

Figure 1. Close-range image pair taken with forward-photographing cameras No.1 (left) and No. 2 (right)

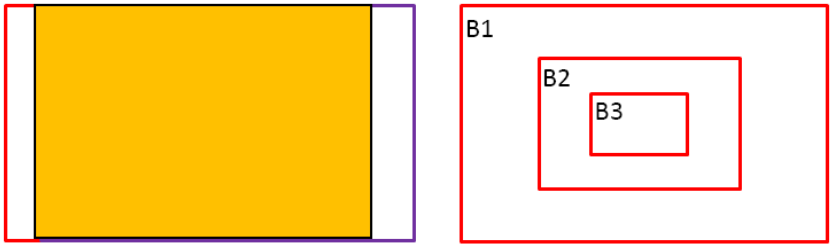

(a) (b)

Figure 2. (a) Synchronously photographed image1 and image2 have circa 90% overlap, (b) the overlap of successive images taken with the same camera is about 60%

In vertical photogrammetry, the aircraft's flight direction is normally perpendicular to the optical axis of aerial camera. However, in the case studied here, the optical axes of our both MMS forward-photographing cameras parallel approximately the driving direction of the MMS van. Both cameras No. 1 and No. 2 take synchronously images with about 90% overlap, as shown in Figure 2(a). There are in total 25 pairs of images taken with both cameras No. 1 and No. 2. The distance between two successive photographing stations is about 2.8m, and the overlap of successive images taken with the same camera on different van locations is about 90%. In order to reduce the number of highly overlapping images and to increase the geometry strength of photogrammetric networks, 9 pair of images are selected as test images from 25 pairs. Therefore, the distance between two successive exposure stations is increased from 2.8m to 8m. Also, the overlap of successive test images taken with the same camera on different van locations is about 60%, as shown in Figure 2(b). Figure 3 shows the feature points extracted by the technique of scale invariant feature transform (SIFT) (Lowe, 1999; Lowe 2004), where neighboring points are illustrated with different color to differentiate from each other. Figure 4(a) shows the locations of the 4 full control points and 29 full check points in the test area of about 91m (ΔY) x 20m (ΔX). The locations of the 18 exposure stations are illustrated in Figure 4(b). Both X and Y axes parallel the coordinate axes of the Taiwan datum TWD97 system. The MMS forward-photographing direction is approximately parallel to the Y axis. Therefore, the quality of object coordinates is worst in Y.

3. TEST RESULTS

The following three sections show briefly the results of three types of tests. All are computed by means of bundle block adjustment with 1. the data snooping process (Baarda, 1968) for blunder detection and deletion, and 2. tuning the a priori standard deviations σ of observations, namely adjusting their weights, so that the ratio of a posteriori standard deviations $\hat{\sigma}$ of observations divided by σ be one, namely $\hat{\sigma}/\sigma=1$. The unknowns in all

computations are 1. ground coordinates of object points, and 2. exterior orientation parameters of all images. Moreover, the root mean square value D_{RMS} of the differences between the known ground coordinates of check points and the ones computed by bundle block adjustment on all check points is calculated and used to evaluate the quality of ground coordinates of object points.

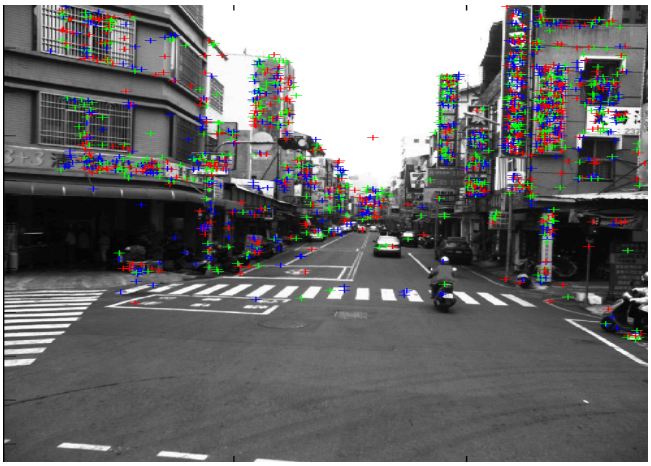

Figure 3. Feature Points extracted by SIFT

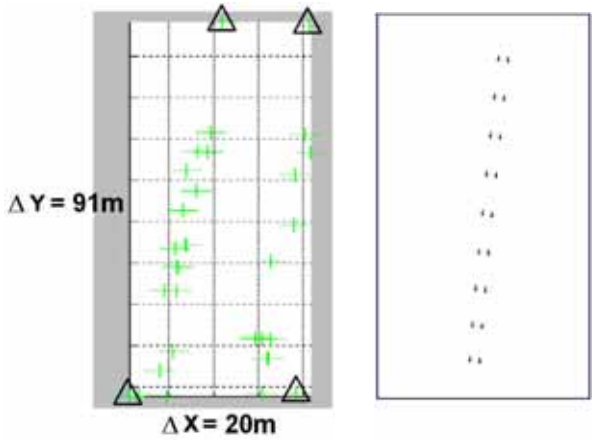

(a) (b)

Figure 4. (a) 4 full control points and 29 full check points in the test area, (b) Locations of the 18 exposure stations

3.1 DISTRIBUTION OF GCPS VERSUS POSITIONING ACCURACY

This section studies the relationship between the distribution of full ground control points (GCPs) and the accuracy of object coordinates. When adding different number of full control points, the AT results are analyzed and checked the applicability for the cartography of 1/1000 maps. The test area of 91m x 20m is a long and narrow region, so that 3 and 4 full control points on the three and four corners, as shown in Figures 5(a) and 5(b), are first adopted. After having 4 full control points on the four corners, different number of full control points are added, as shown in Figure 5(c)~5(f). These six tests are named the examples c1~c6, respectively.

Figure 6 shows the D_{RMS} of X, Y and Z components in the cases c1~c6. It shows clearly that the case with more full control points has a better accuracy, namely smaller D_{RMS}. The cases c1 and c2 have the D_{RMS} 52.2cm and 40.2mm respectively. In the cases c3~c6, the D_{RMS} on check points is reduced significantly to 16.3cm ~ 22.6cm.

3.2 ADDING GPS/IMU DATA VERSUS POSITIONING ACCURACY

The following eight tests are all done with the observations of exterior orientation parameters provided by GPS/IMU data. The test d1 uses only GPS/IMU data as constraints in the photo triangulation. Figure 7 illustrates the locations of a full control point and check points adopted in the test d2. The other tests d3~d8 utilize the same full control points and check points as the aforementioned tests c1~c6, respectively.

The tests d1 and d2 have the D_{RMS} of 88.1cm and 33.1cm, respectively. The D_{RMS} values range from 13.7cm to 15.6cm in the other tests d3~d8. Figure 8 shows the D_{RMS} values of X, Y, Z components in the cases d1~d8. They demonstrate that the MMS forward-photographed images have the applicability potential for cartography of 1/1000 maps when using GPS/IMU data together with at least one full control point as constraints for photo triangulation.

The error ellipses of object coordinates determined by photo triangulation are also computed and illustrated in Figure 9, where the scales for drawing the error ellipses in tests d1~d3 are the same, and shown on the bottom of

the figures 9(a)~9(c). For the computation of error ellipses please refer to (Wolf and Ghilani, 1997). A difference vector on a check point is defined as a vector from the known location to the one determined by photo triangulation. Figure 10 show the difference vectors on the check points in the tests d1~d3, where all have the same vector scale. Both error ellipse maps and the difference vector maps of the tests d4~d8 are similar with the ones of the test d3 so that they are not shown. The test d1 has the average semi-major axis length greater than 90.0cm, but after adding a GCP, the average semi-major axis length is significantly reduced to about 9.5cm in the test d2. When adding more GCPs in the tests d3~d8, the average length of semimajor axes of error ellipses ranges from 5.8cm to 6.9cm, and the ratio of semimajor to semiminor axis length is 3:1.

Figure 10(a) shows apparently that systematic larger horizontal and vertical difference vectors exist on all check points in the test d1. But, these vectors become significantly much shorter and more randomly after adding one GCP in the test d2. Some local vectors in the test d2 exhibit systematic direction and length. The average $|D_X|$, $|D_Y|$ and $|D_Z|$ values are reduced from 72.0cm, 36.5cm, 28.3cm in the test d1 to 8.5cm, 10.2cm, 20.4cm in the test d2. In the tests d3~d8, the average $|D_X|$, $|D_Y|$ and $|D_Z|$ are 3.1cm~3.6cm, 9.0cm~11.0cm, 2.7cm~3.1cm, respectively.

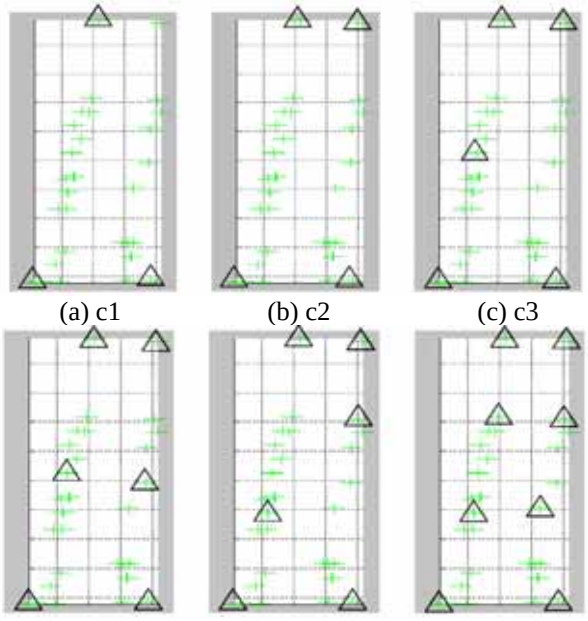

(a) c1 (b) c2 (c) c3

(d) c4 (e) c5 (f) c6

Figure 5 Locations of different number of full control points Δ and check points + in the tests c1~c6

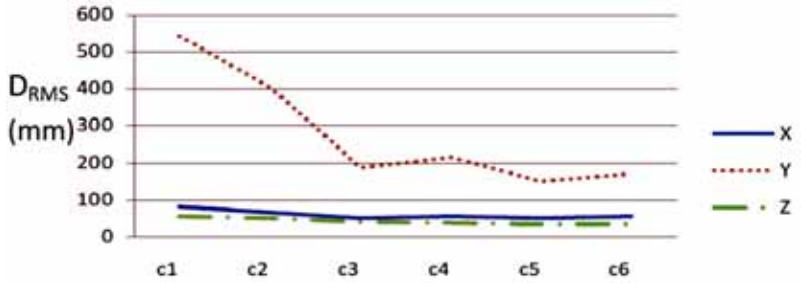

Figure 6 The D_{RMS} of X, Y, Z components in the cases c1~c6

3.3 POINT POSITIONING QUALITY IN TOPOGRAPHY MAP UPDATING CASES

In any application case for updating 1/1000 topographic maps on a MMS, only a few images pairs and less image points are adopted. In the following three tests, 2, 4 and 6 images taken on three successive stations with the distance interval of about 8m are adopted. All cases apply GPS/IMU data as constraints for photo triangulation. Figure 11 shows the D_{RMS} of X, Y, Z components in the three cases without any GCP. When only GPS/IMU data are used as constraints in the photo triangulation, the point positioning results don't satisfy the accuracy requirement for cartography of 1/1000 maps. But, after adding one GCP, the horizontal and vertical D_{RMS} values are 25.4cm and 7.0cm in the case with four images. If six images taken on three successive stations are used, the horizontal and vertical D_{RMS} values are 24.0cm and 4.5cm, respectively. Both cases with four and six images demonstrate that the successive forward-photographed images are available for cartography of 1/1000 maps.

4. CONCLUSIONS

This paper studies briefly the quality of MMS forward-photographed image intersection. All tests conclude that close-range photogrammetry using forward-photographed images taken on a MMS van can satisfy the need on the accuracy requirement for cartography of 1/1000 maps, if proper constraints are adopted. In our test area of 91m x 20m along a street, the horizontal and vertical accuracy represented by D_{RMS} values on check points are 25.4cm and 7.0cm, when one adopts four images taken on two successive stations with the distance interval of 8m and on two forward-photographing cameras with the baseline length 1.65m, where GPS/IMU data together with a GCP are utilized.

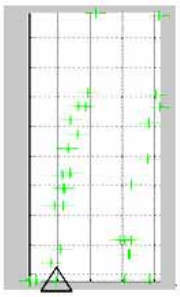

Figure 7 Locations of a full control point and check points adopted in the test d2

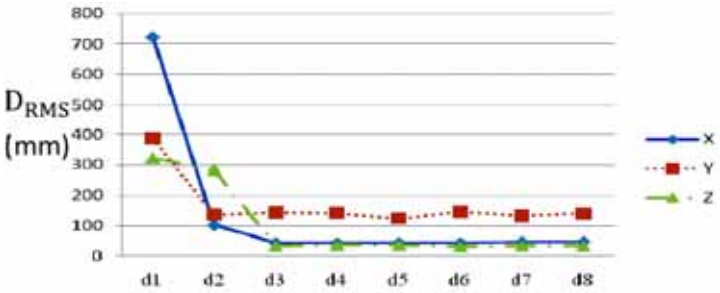

Figure 8 The D_{RMS} of X, Y, Z components in the cases d1~d8

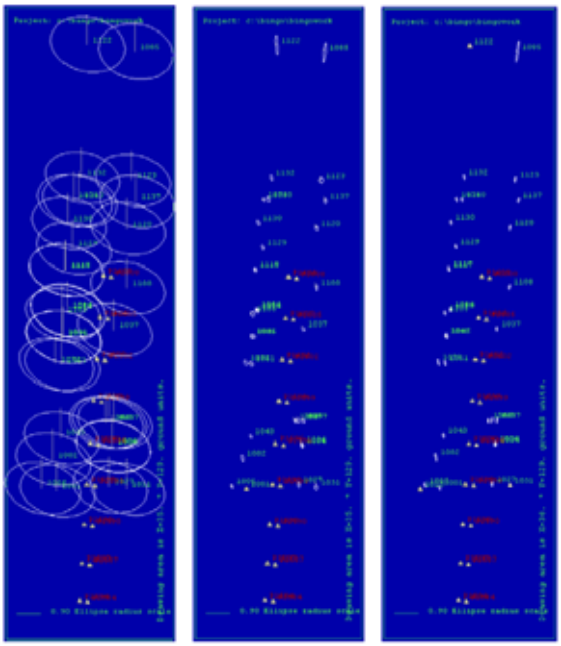

(a) d1 (b) d2 (c) d3

Figure 9 The error ellipses in the tests d1~d3

REFERENCE

Baarda, W., 1968. A Testing Procedure for Use in Geodetic Networks, Netherlands Geodetic Commission, Vol. 2, No. 5.

El-Sheimy, N., 1996. The Development of VISAT - A Mobile Survey System For GIS Applications, UCGE Report #20101, Department of Geomatics Engineering, The University of Calgray, Canada.

Ellum, C. and EI-Sheimy, N., 2002. Land-based mobile mapping systems, Photogrammetric Engineering and Remote Sensing, Vol. 68, No. 1, pp. 13-28.
Lee, H. K., Hewitson, S., Wang, J., 2004. Web-based resources on GPS/INS integration, GPS Solutions, Vol. 8, pp. 189-191.
Lowe, D.G. 1999. Object recognition from local scale-invariant features, In International Conference on Computer Vision, Corfu, Greece, pp. 1150-1157.
Lowe, D. G., 2004. Distinctive image features from scale-invariant keypoints, International Journal of Computer Vision, Vol. 60, No. 2, pp. 91-110.
Wolf, P. R. and Ghilani, C. D., 1997, Adjustment Computations: Statistics and Least Squares in Surveying and GIS, John Wiley & Sons.

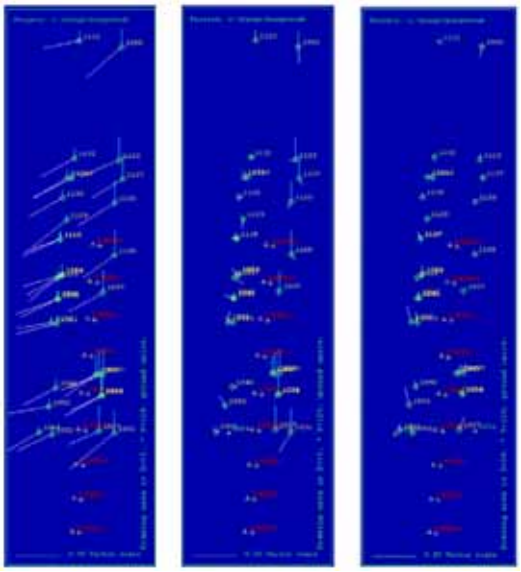

(a) d1 (b) d2 (c) d3

Figure 10 The difference vectors on the check points in the tests d1~d3

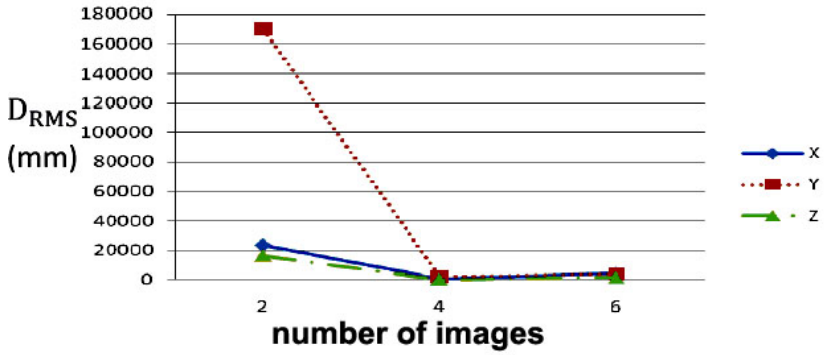

Figure 11 The D_{RMS} of X, Y, Z components in the three cases without any GCP

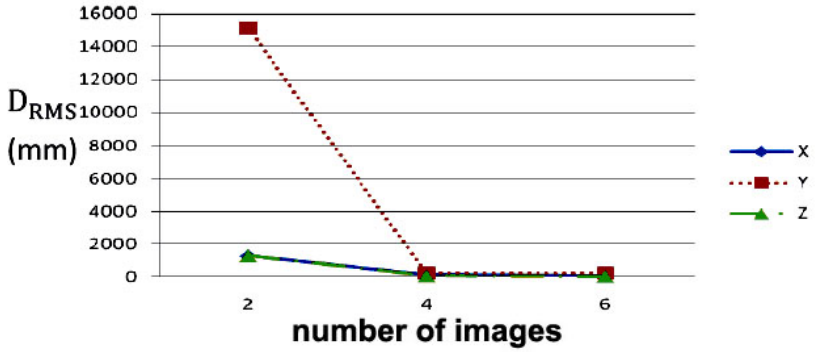

Figure 12 The D_{RMS} of X, Y, Z components in the three cases with a GCP